

Biophysical Interactions of Novel Oleic Acid Conjugate and its Anticancer Potential in HeLa Cells

Azmat Ali Khan · Amer M. Alanazi · Mumtaz Jabeen · Khalid Pervez · Rizwan Wahab · Ali Saber Abdelhameed · Arun Chauhan

Received: 11 September 2014 / Accepted: 19 January 2015 / Published online: 1 February 2015
© Springer Science+Business Media New York 2015

Abstract Novel conjugate 2,6-Diisopropylphenol-Oleic acid (2,6P-OLA) has shown potent anticancer activity on various cancer cell lines (Khan et al. *Lipids* 47:973–986, 2012). In the present study, the protein-or/ and DNA-binding property of 2, 6P-OLA was evaluated that could predict its potential toxic effect, in vitro. Preferential structural stability and interaction mechanism of 2,6P-OLA to human serum albumin (HSA) and calf thymus DNA (CT-DNA) was used as model molecules, employing fluorescence spectroscopy (FS) and circular dichroism (CD) methods. The binding and apoptotic activities of conjugate were determined on bacterial recombinant DNA, pBR322 and human cancer cell line, HeLa, respectively. FS studies showed a strong conjugate binding affinity to HSA with overall binding constant of $K=7.66 (\pm 0.03) \times 10^2 \text{ M}^{-1}$. Higher concentration induced detectable changes in the CD spectrum of HSA. The conjugate complexation altered HSA secondary conformation by an increase in α -helices and decrease in β -sheets. Fluorescence quenching studies with CT-

DNA exhibited $K=1.215 \times 10^2 \text{ L mol}^{-1}$ where 2,6P-OLA efficiently displaced the ethidium bromide (EtBr) bound DNA indicating its strong competition with EtBr for intercalation. Similarly, 2,6P-OLA was able to partially bind pBR322, resulting in decrease the intensity of EtBr gradually. The conjugate significantly reduced survival of HeLa cells. Morphological studies revealed altered cell morphology, suggesting apoptotic death of HeLa cells. Overall, our data shows that 2,6P-OLA bind well with both HSA and DNA and possessed anticancer activities.

Keywords Fluorescence · 2,6-Diisopropylphenol-Oleic acid · HeLa cancer cells · Circular dichroism · Cytotoxicity

Introduction

For effective targeting of any of the newly synthesized drug/conjugate, an understanding of its modes of action is a necessity that can be achieved by studying its interactions with proteins, hormones, peptides, deoxyribonucleic acid etc. 2,6-Diisopropylphenol-Oleic acid (2,6P-OLA); is a novel oleic acid conjugate that possess potent antineoplastic properties. Because of its inhibitory and apoptotic action on cancer cells, in vitro [1], it has a potential of being characterised as a member of a new class of fatty acid based anticancer agents [2–7]. 2,6P-OLA as of now, has not been exploited for its interaction abilities with various biological targets. In the present study, we have tried to evaluate the mechanism of action of 2,6P-OLA at the protein and molecular level that will probably predict its plausible effect as an anticancer agent.

Drug-protein interaction is an important pharmacological parameter that helps in elucidating the metabolism, distribution and transportation of a drug [8]. Among proteins, serum albumin is the principal extracellular protein of the circulatory system that has been extensively studied. It functions as a

A. A. Khan (✉) · A. M. Alanazi · A. S. Abdelhameed
Department of Pharmaceutical Chemistry, College of Pharmacy,
King Saud University, Riyadh 11451, Kingdom of Saudi Arabia
e-mail: azmatbiotech@gmail.com

M. Jabeen
Section of Genetics, Department of Zoology,
Aligarh Muslim University, Aligarh 202002, India

K. Pervez
Department of Pharmacognosy, College of Pharmacy,
King Saud University, Riyadh 11451, Kingdom of Saudi Arabia

R. Wahab
Department of Zoology, College of Science, King Saud University,
Riyadh 11451, Kingdom of Saudi Arabia

A. Chauhan
Department of Neuroimmunology, School of Health and Medicine,
University of North Dakota, Grand Forks, ND, USA

physiological carrier for numerous endogenous and exogenous compounds such as fatty acids, amino acids, steroids, metal ions, and drugs [9–11]. Human serum albumin (HSA) is a single chain 66 kDa non-glycosylated α -helical polypeptide. The presence of aromatic amino acids provides HSA inherent property to fluoresce. HSA has also shown varied binding affinities, for instance, the weak binding result in poor distribution and strong binding decrease the concentration of free drug in plasma [12] and, improve the pharmacodynamics and pharmacokinetics of the biomolecule [13]. These important properties make HSA, a preferred target protein molecule for exploring the fate of bound molecule. Besides HSA, deoxyribonucleic acid (DNA) is also a primary intracellular target molecule upon which most of the anticancer drugs exert their cytotoxic effects [14, 15]. Drug or small molecules react with DNA mostly through non-covalent interactions on several sites in the DNA molecule. Based on interaction site, compounds can intercalate between two base pairs or bind with minor and major groove or can show electrostatic binding [16]. Most of the DNA interacting molecules like intercalators, groove binders and alkylating compounds act as an antitumor agents [17, 18]. The mode of binding of drug/compound with DNA will therefore help in understanding the action mechanism of DNA targeted antitumor drugs.

In the present study, the interaction of conjugate with HSA, calf thymus DNA (CT-DNA) and pBR322 DNA in aqueous solution at physiological conditions has been evaluated employing fluorescence spectroscopy (FS), circular dichroism (CD) and electrophoretic methods. The study, also deals with cytotoxic and apoptotic activities of 2,6P-OLA on HeLa cancer cells.

Materials and Methods

Chemicals

Fat free human serum albumin (HSA), calf thymus DNA (sodium salt, average molecular weight 1×10^6), RPMI 1640 medium, fetal bovine serum (FBS), MTT dye, trypsin EDTA solution, ethidium bromide, Tris base (Tris-(hydroxymethyl)-amino-methane-hydrogen chloride) and agarose were purchased from Sigma-Aldrich (St. Louis, MO, USA). All other chemicals used for analysis were also from Sigma-Aldrich (St. Louis, MO, USA).

Cell Culture

HeLa cells (Human cervical carcinoma) were obtained from the American Type Culture Collection (Rockville, MD). The cells were maintained in RPMI 1640 medium containing 10 % (v/v) heat-inactivated FBS, 2 mM L-glutamine, 100 U/ml

penicillin and 100 μ g/ml streptomycin at 37 °C in a 95 % humidified atmosphere containing 5 % CO₂.

Preparation of Stock Solutions

A stock solution of 5 mM of 2,6P-OLA (in ethanol) was prepared in 10 mM Tris-HCl and further diluted to various concentrations in the same buffer. As already reported [19], a solution containing low amounts of ethanol does not affect the secondary structure of HSA. A stock solution of 0.5 mM HSA was prepared in aqueous solution containing 10 mM Tris-HCl (pH 7.4) and equilibrated overnight. The protein concentration was spectrophotometrically determined on NanoDrop 2000 (Thermo Scientific, USA). Calf thymus DNA (CT-DNA) solution of 1 mg/ml was dissolved in 10 mM Tris-HCl (pH 7.4) and stored at 4 °C. UV absorbance values of approximately 1.89:1 (A₂₆₀: A₂₈₀ nm) of CT-DNA solutions indicates DNA to be satisfactorily protein-free [20]. Ethidium bromide (EtBr) solution of 1 mg/ml was dissolved in 10 mM Tris-HCl (pH 7.4) and stored at 4 °C. The working standard solutions of the complexes were prepared freshly when used.

Fluorescence Measurements

Fluorescence emission spectra were recorded on Jasco FP-8200 fluorescence spectrophotometer with a constant temperature-holder and 1 cm path length cell. The excitation and emission slits were set at 5 and 10 nm, respectively. Intrinsic fluorescence for the HSA-conjugate complex was measured by exciting the protein solution at λ_{exc} 295 nm. The emission (λ_{em}) was recorded from 300 to 400 nm. Intrinsic fluorescence for CT-DNA-conjugate complex was measured by exciting the DNA solution at λ_{exc} 395 nm and recording λ_{em} from 395 to 530 nm.

2,6P-OLA and HSA were incubated for 10 min maximum for forming complexes. A fixed HSA concentration of 20 μ M and 1–100 μ M increasing concentrations of conjugate was used. For the interaction of conjugate with CT-DNA, initially, 10 μ l of EtBr was mixed with 30 μ l of CT-DNA, and then increasing concentrations of 2,6P-OLA from 1 to 10 μ M was used for recording the emission spectra. Considering the maximum binding time of 1 h after standardizing via UV-vis absorption, the conjugate and CT-DNA-EtBr were incubated for 1 h maximum for all the experiments. The Stern-Volmer constant values were calculated from averages of four replicate runs for the conjugate-HSA/ conjugate-DNA complexes at different concentrations of conjugate. All experiments were conducted at 25 ± 1 °C.

Circular Dichroism Measurements

CD spectra were recorded on Jasco J-815 spectropolarimeter. Spectra were collected with 50 nm/min scan speed, 0.1 nm

data pitch and a response time of 2 s. Each spectrum was the average of 3 scans. For measurements in the far-UV region (190–250 nm), a quartz cell with a path length of 0.1 cm was used. Far-UV CD spectra were recorded by incubating HSA at a fixed concentration of 20 μM with three different concentrations of 2,6P-OLA viz., 10, 20 and 40 μM.

pBR322 DNA Interaction Studies

Interaction between 2,6P-OLA and pBR322 DNA was visualized on agarose gel electrophoresis. Increasing concentrations of conjugate (1–10 μM) were added to the DNA (0.5 μg/ 500 μl) in TE (10 mM Tris–HCl, 0.1 mM EDTA, pH 7.4) buffer solution. After incubating each reaction mixture for 2 h at 37 °C, the reaction was stopped by the addition of sample loading buffer. The aliquots from each sample were electrophoresed on 0.8 % agarose gel. After electrophoresis, gels were stained with ethidium bromide and visualized on Alpha Imager gel documentation system (ProteinSimple, CA, USA).

Cell Proliferation Assay

The proliferation of HeLa cells was assessed using MTT assay according to Mosmann [21]. Briefly, 5 × 10⁵ cells/ well in exponential growth were seeded into 96-well plates and were treated with increasing concentration of 2,6P-OLA from 0 to 15 μM [1]. After 94 h, MTT reagent (5 mg/ml PBS) was added to each well at the ratio of 1:10 (v/v). Absorbance was measured at 620 nm in a multi-well plate reader. Drug sensitivity was expressed in terms of the concentration of 2,6P-OLA required for a 50 % reduction in cell survival (IC₅₀).

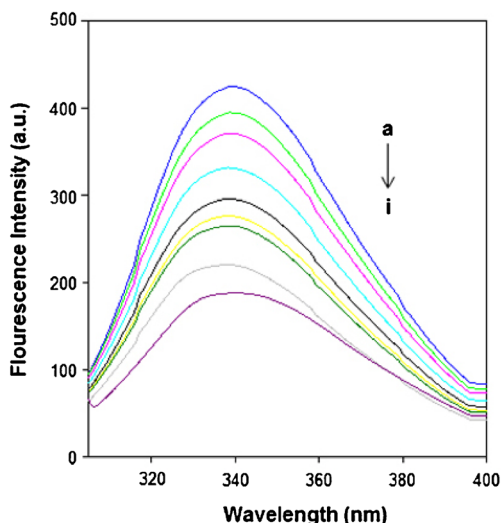


Fig. 1 Fluorescence emission spectra of 2,6P-OLA-HSA complex in 10 mM Tris–HCl (pH 7.4) excited at 295 nm. There was a decrease of HSA fluorescence during the binding with the conjugate at 1, 5, 10, 15, 20, 30, 40 and 50 μM

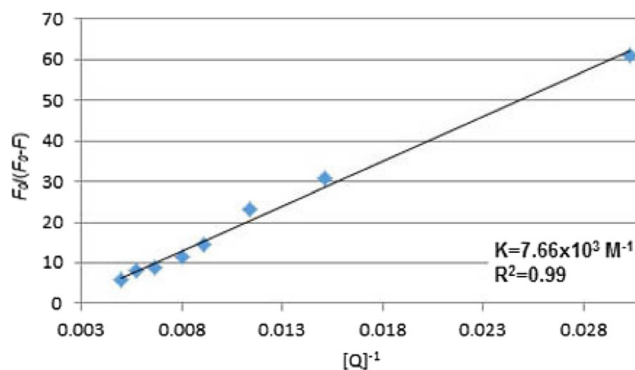


Fig. 2 Stern-Volmer plot of $F_0/(F_0-F)$ as a function of $1/(2,6P-OLA)^{-1}$ in the determination of the fluorescence quenching constant (K) for the conjugate during binding at different concentrations with HSA

Microscopy Studies

The cells were seeded in 6-well plates and allowed to adhere at 37 °C in CO₂ incubator. After 24 h, each well was treated with 4.6 μM 2,6P-OLA and incubated for the indicated time. After 12 and 24 h, the cells were imaged by phase contrast microscope (Olympus CLX 41) to visualize morphological changes in HeLa cells.

Results and Discussion

Fluorescence Quenching of HSA in Presence of 2,6P-OLA

When a drug binds with serum albumin, it undergoes various pharmacological changes like increased solubility in plasma, decreased toxicity and protection against oxidation. Moreover, strong binding of drug stops its release in tissues [22]. In the present study, the level of interaction of 2,6P-OLA

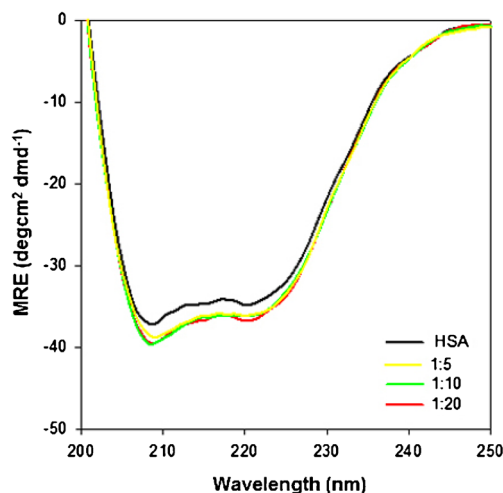


Fig. 3 The changes of Far-UV CD spectra of HSA in the presence of 2,6P-OLA. CD spectra were recorded at three different molar ratios of HSA vs conjugate viz., 1:5, 1:10 and 1:20

with HSA was determined by FS. The fluorescence of HSA comes from the tryptophan, tyrosine, and phenylalanine residues. Actually, the intrinsic fluorescence of HSA is almost contributed by tryptophan alone, because phenylalanine has a very low quantum yield and the fluorescence of tyrosine is almost totally quenched if it is ionized or near an amino or a carboxyl group, or a tryptophan. This viewpoint is well supported by the experimental observation of Sulkowska [23]. This implies, the change of intrinsic fluorescence intensity of the HSA is that of a tryptophan residue when small molecule substances bind to HSA. HSA alone shows a strong fluorescence emission band at 340 nm while 2,6P-OLA has no intrinsic fluorescence at the excitation wavelength of 280 nm. Figure 1 shows the fluorescence emission spectra of HSA in the absence and in presence of different concentrations of 2,6P-OLA. The fluorescence emission intensity of HSA decreases gradually with the increase of concentration of 2,6P-OLA, depicting that emission intensity is quenched in a concentration-dependent manner (Fig. 1). The strong quenching of the HSA fluorescence also indicates that the microenvironment around Trp 214 residue changes after the addition of the conjugate.

The quenching data from the fluorescence titration experiments was analyzed according to the modified Stern-Volmer equation [24].

$$F_0/(F_0-F) = 1/fK[Q] + 1/f$$

Where F_0 and F are the relative fluorescence intensities of HSA in the absence and presence of quencher, respectively; K is the Stern-Volmer binding constant; $[Q]$ is the quencher concentration and f is the fractional maximum fluorescence

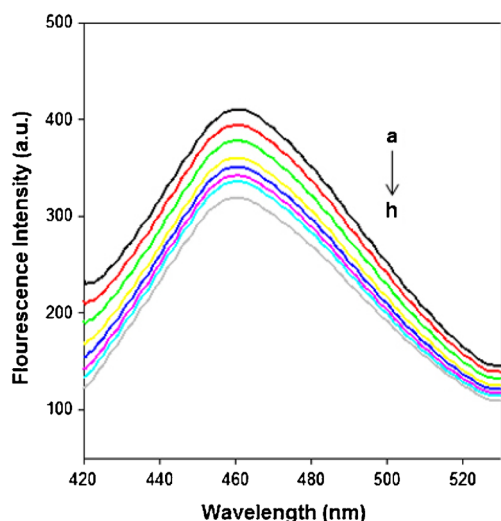


Fig. 4 Fluorescence emission spectra of 2,6P-OLA-CT-DNA complex in 10 mM Tris-HCl (pH 7.4) excited at 395 nm. The decrease of EtBr-CT-DNA fluorescence during the binding with the conjugate from 1 to 10 μ M show a competition between conjugate and EtBr

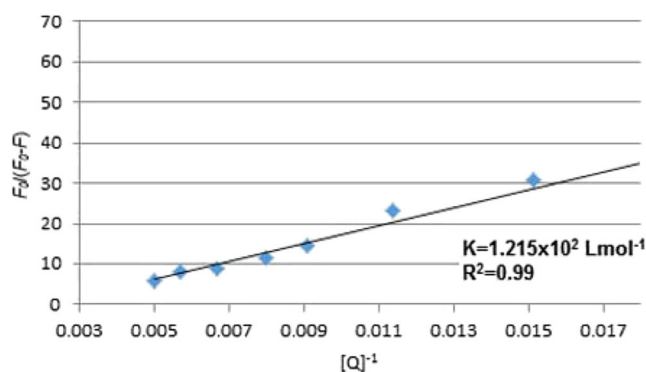


Fig. 5 Stern-Volmer plot of $F_0/(F_0-F)$ as a function of $1/(2,6P-OLA)^{-1}$ in the determination of the fluorescence quenching constant (K) for the conjugate during binding at different concentrations with EtBr-CT-DNA

intensity of the protein summed up. Binding constant K is a quotient of intercept $1/f$ and slope ($1/fK$). The obtained $K=7.66 (\pm 0.03) \times 10^2 \text{ M}^{-1}$ is comparatively high binding constant suggesting that 2,6P-OLA is a better ligand for HSA [13, 25, 26]. The plot of $F_0/(F_0-F)$ versus $1/[Q]$ shows good upward linear relationship ($r=0.998$) (Fig. 2) indicating the binding between 2,6P-OLA and HSA complex to be mainly static [27].

Change in Secondary Structure of HSA in Presence of 2,6P-OLA by far-UV CD

To study the effect of 2,6P-OLA on the conformational changes in secondary structure of HSA, molar ratios of 1:5, 1:10 and 1:20 for HSA to conjugate were taken. The results were expressed as MRE (mean residue ellipticity) in $\text{deg.cm}^2.\text{dmol}^{-1}$, which is given by:

$$MRE = \theta_{obs}(\text{mdeg})/Cpl \times 10$$

Where θ_{obs} is the observed ellipticity in degrees, C_p is the molar fraction, n is the number of amino acid residues and l is the length of the light path in centimeter [28]. The protein secondary structure was calculated using CDNN 2.1 software. Figure 3 shows the CD spectra of HSA in the absence and presence of conjugate. The CD spectra of HSA exhibit two negative peaks in the ultraviolet region at 209 and 222 nm, which is a characteristic of α -helical structure [29]. The

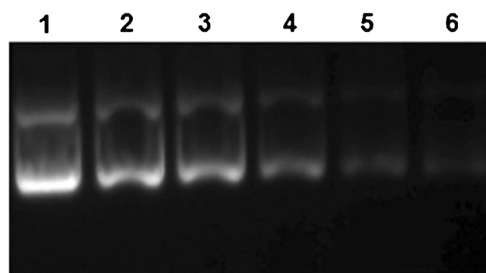


Fig. 6 Binding studies of pBR322 DNA in the presence of 2,6P-OLA. Lane 1: control, Lane 2–6: 1, 2, 4, 6, 10 μ M concentration of the conjugate

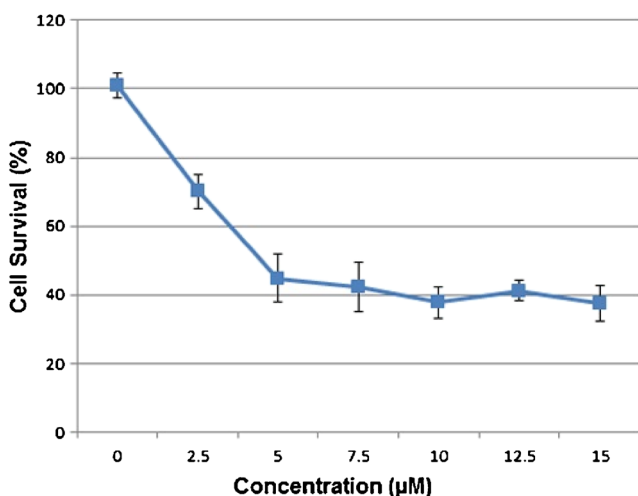


Fig. 7 Dose-dependent viability curve of HeLa cells after treatment with 2,6P-OLA. Viability was checked by MTT assay after 48 h

present data also shows the presence of two negative peaks of the HSA at its original position. However, the tested molar ratios of HSA-conjugate complex resulted in change of α -helical content of the protein. It was observed that upon binding with 2,6P-OLA % α -helices increased from 60.98 % in the native HSA to 62.25, 63.10 and 63.98 % with an increase in molar ratios (1:5, 1:10, 1:20, respectively). Similarly, % β -sheets in complex slightly reduced from 4.02 % in native HSA to 3.68, 2.65 and 2.02 % with an increase in molar ratios (1:5, 1:10, 1:20, respectively). This confirms that, with the increase in concentration of conjugate, interaction with HSA causes a slight increase in the ellipticity. Because of this HSA undergoes folding at high conjugate concentrations which can be probably due to the electrostatic binding of the conjugate to the exposed binding sites of HSA [30].

Fluorescence Quenching of CT-DNA in the Presence of 2,6P-OLA

In order to investigate the interaction modes between 2,6P-OLA and DNA, the ethidium bromide (EtBr) fluorescence displacement experiments were used. Upon excitation, 2,6P-OLA is non-emissive in aqueous solution. In general, the

intrinsic fluorescence intensity of DNA is also very low, and that of EtBr in solution is also not high due to quenching by the solvent molecules. However, upon addition of DNA, the fluorescence intensity of EtBr enhances because of its intercalation into the DNA. Moreover, when EtBr is displaced from its intercalation site there is 24-fold decrease in its fluorescence [31]. Thus, EtBr is suitably used as a reporter to probe the interaction of drug with DNA.

In the present study, as illustrated in Fig. 4, the fluorescence emission spectra significantly increased upon addition of EtBr to CT-DNA. When increasing concentration of conjugate was added to CT-DNA-EtBr complex the fluorescence intensities of EtBr bound to CT-DNA showed a remarkable decreasing trend at 460 nm. The decrease in spectra indicates that some EtBr molecules were released into solution after an exchange with the conjugate resulting in the fluorescence quenching of EtBr. The obtained value of binding constant K is equal to $1.215 \times 10^2 \text{ L mol}^{-1}$ depicting the magnitude of the binding strength. Figure 5 shows the Stern-Volmer plot where good upward linear relationship ($r=0.996$) is seen upon binding CT-DNA with increasing concentration of conjugate. The fluorescence intensity of EtBr is quenched by the addition of conjugate due to the decrease in the binding sites of DNA available for EtBr [32]. Since EtBr interacts with DNA through intercalation into the minor groove, its displacement by compound indicates an intercalative type of binding [33] where conjugate intercalates into the adjacent base pairs of DNA easily.

Interaction of 2,6P-OLA With pBR322 Plasmid DNA

The interaction of the conjugate was also studied on pBR322 plasmid DNA using agarose gel electrophoresis. pBR322 at fixed concentration was incubated with different concentrations from 1 to 10 μM of 2,6P-OLA. After incubation, aliquots of 10 μl were run on 0.8 % agarose gel. In Fig. 6; with increase in concentration of the conjugate (lanes 1–6), the intensity and mobility of plasmid DNA decreases. This decrease in EtBr intensity supports the fluorescent spectroscopy observations. The conjugate acts as an intercalator where it replaces EtBr and effectively binds with the plasmid DNA at as low as 1 μM .

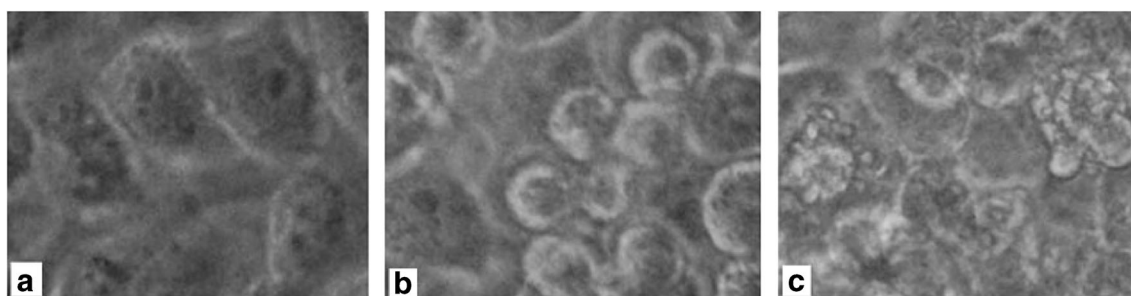


Fig. 8 Morphological changes in HeLa cells treated with 2,6P-OLA. **a** untreated cells, **b** cells after 12 h and **c** cells after 24 h

Cytotoxic Effects of 2,6P-OLA on HeLa Cells

Cancer HeLa cells were treated with increasing concentration of conjugate. As shown in Fig. 7, the conjugate has a significant inhibitory effect ($p < 0.05$) on the growth of HeLa cells in a dose-dependent manner. The IC_{50} value of 4.6 μM clearly marks the potent nature of 2,6P-OLA on HeLa cells. The cytotoxic effect of conjugate on HeLa cells is in agreement with its previously reported results on other cancer cell lines [1]. The structural modifications of propofol and oleic acid impart extra edge on the final product, thereby placing it in a class of anticancer agents depicting selectivity and specificity.

Morphological Changes

HeLa cells after treatment with 2,6P-OLA were studied for morphological variations using phase contrast microscopy. Changes in surface morphology were observed after 12 and 24 h (Fig. 8). Many characteristic features occur in cell undergoing series of biochemical events during apoptosis. Various morphological changes like blebbing, loss of membrane asymmetry, cell shrinkage, nuclear fragmentation, chromatin condensation, and chromosomal DNA fragmentation occur. In Fig. 8b, cells exposed to 4.6 μM of conjugate for 12 h shows the onset of apoptotic characteristics where most of the cells lose their typical branch shaped morphology and cause shrinking of cell. After 24 h exposure (Fig. 8c), blebbing and loss of basal attachment and membrane asymmetry is markedly seen.

Conclusion

The present spectrofluoroscopic results suggest that 2,6P-OLA binds well with both HSA and CT-DNA. Conjugate-HSA binding shows the formation of more stable complexes but at high conjugate concentrations, HSA undergoes slight conformational change due to increase in ellipticity. 2,6P-OLA acts as an intercalator where it replaces EtBr and binds with CT-DNA as well as the plasmid DNA. Moreover, the conjugate is able to significantly inhibit the growth of HeLa cells and acts as the basis of apoptotic activities in cancer cells. Hence, the current study regarding protein-or/and DNA-binding interaction of 2,6P-OLA helps in elucidating the important aspect of its pharmacokinetics.

Acknowledgments Authors would like to extend their sincere appreciation to the Deanship of Scientific Research at King Saud University for funding of this research through the Research Group Project No. RGP-212.

Conflict of Interest Authors have no conflict of interest.

References

1. Khan AA, Husain A, Jabeen M, Mustafa J, Owais M (2012) Synthesis and characterization of novel n-9 fatty acid conjugates possessing antineoplastic properties. *Lipids* 47:973–986
2. Harvey KA, Xu Z, Whitley P, Jo Davison V, Siddiqui RA (2010) Characterization of anticancer properties of 2,6-diisopropylphenol-docosahexaenoate and analogues in breast cancer cells. *Bioorg Med Chem* 18:1866–1874
3. Khan AA, Alanazi AM, Jabeen M, Chauhan A, Abdelhameed AS (2013) Design, synthesis and in vitro anticancer evaluation of a stearic acid-based ester conjugate. *Anticancer Res* 33:2517–2524
4. Manendez JA, Ropero S, Lupu R, Colomer R (2004) Omega-6 polyunsaturated fatty acid gamma-linolenic acid (18:3n-6) enhances docetaxel (taxotere) cytotoxicity in human breast carcinoma cells: relationship to lipid peroxidation and HER-2/neu expression. *Oncol Rep* 11:1241–1252
5. Khan AA, Jabeen M, And KAA, Owais M (2013) Anticancer efficacy of a novel propofol-linoleic acid-loaded escheriosomal formulation against murine hepatocellular carcinoma. *Nanomedicine* 8: 1281–1294
6. Siddiqui RA, Zerouga M, Wu M, Castillo A, Harvey KA, Zaloga GP, Stillwell W (2005) Anticancer properties of propofol-docosahexaenoate and propofol-eicosapentaenoate on breast cancer cells. *Breast Cancer Res* 7:645–654
7. Khan AA, Alam M, Tufail S, Mustafa J, Owais M (2011) Synthesis and characterization of novel PUFA esters exhibiting potential anticancer activities: an in vitro study. *Eur J Med Chem* 46:4878–4886
8. Chakrabarty A, Mallick A, Haldar B, Das P, Chattopadhyay N (2007) Binding interaction of a biological photosensitizer with serum albumins: a biophysical study. *Biomacromol* 8:920–927
9. Peters T Jr (1985) Serum albumin. *Adv Protein Chem* 37:161–245
10. He XM, Carter DC (1992) Atomic structure and chemistry of human serum albumin. *Nature* 358:209–215
11. Quevedo MA, Moroni GN, Brinon MC (2001) Human serum albumin binding of novel antiretroviral nucleoside derivatives of AZT. *Biochem Biophys Res Commun* 288:954–960
12. Cheema MA, Taboada P, Barbosa S, Castro E, Siddiq M, Mosquera V (2007) Modification of the thermal unfolding pathways of myoglobin upon drug interaction in different aqueous media. *J Phys Chem B* 111:13851–13857
13. Ruan BF, Huang XF, Ding H, Xu C, Ge HM, Zhu HL, Tan RX (2006) Synthesis and cytotoxic evaluation of a series of resveratrol derivatives. *Chem Biodivers* 3:975–981
14. Coleman RS, Perez RJ, Burk CH, Navarro A (2002) Studies on the mechanism of action of azinomycin B: definition of region selectivity and sequence selectivity of DNA cross-link formation and clarification of the role of the naphthoate. *J Am Chem Soc* 124:13008–13017
15. Jiao K, Wang QX, Sun W, Jian FF (2005) Synthesis, characterization and DNA-binding properties of a new cobalt(II) complex: $\text{Co}(\text{bbt})_2\text{Cl}_2$. *J Inorg Biochem* 99:1369–1375
16. Ni Y, Lin D, Kokat S (2006) Synchronous fluorescence, UV-visible spectrophotometric, and voltammetric studies of the competitive interaction of bis(1,10-phenanthroline)copper(II) complex and neutral red with DNA. *Anal Biochem* 352:231–242
17. Maiya BG, Arounagui S, Eswaramoorthy D, Asokkumar A, Dattagupta A (2000) Cobalt(III), nickel(II) and ruthenium(II) complexes of 1,10-phenanthroline family of ligands: DNA binding and photocleavage studies. *Indian Acad Sci* 112:1–17
18. Kumar A, Mitra A, Rao CP, Ajay AK, Bhat MK (2012) Cu(II) complexes of glyco-imino-aromatic conjugates in DNA binding, plasmid cleavage and cell cytotoxicity. *J Chem Sci* 124:1217–1228
19. Kanakis C, Tarantilis P, Polissiou M, Diamantoglou S, Tajmir-Riahi H (2006) Antioxidant flavonoids bind human serum albumin. *J Mol Struct* 798:69–74

20. Liu GD, Liao JP, Fang YZ, Huang SS, Sheng GL, Yu RQ (2002) Interaction of bis(ethylene)tin(bis(salicylidene)ethylenediamine) with DNA. *Anal Sci* 18:391–395
21. Mosmann T (1983) Rapid colorimetric assay for cellular growth and survival: application to proliferation and cytotoxicity assays. *J Immunol Methods* 65:55–63
22. Buxton I (2006) Pharmacokinetics and pharmacodynamics. In: Brunton L, Lazo J, Parker K (eds) *The pharmacological basis of therapeutics*, 11th edn. McGraw-Hill, New York, pp 1–39
23. Sułkowska A (2002) Interaction of drugs with bovine and human serum albumin. *J Mol Struct* 614:227–232
24. Lakowicz JR (2007) *Principles of fluorescence spectroscopy*. 3rd ed. Springer
25. Sun H, Nikolovska-Coleska Z, Yang CY, Xu L, Liu M, Tomita Y, Pan H, Yoshioka Y, Krajewski K, Roller PP, Wang S (2004) Structure-based design of potent, conformationally constrained Smacmimetics. *J Am Chem Soc* 126:16686–16687
26. Park CM, Oie T, Petros AM, Zhang H, Nimmer PM, Henry RF, Elmore SW (2006) Design, synthesis, and computational studies of inhibitors of Bcl-XL. *J Am Chem Soc* 128:16206–16212
27. Tian J, Liu J, Hu Z, Chen X (2005) Binding of the scutellarin to albumin using tryptophan fluorescence quenching, CD and FT-IR spectra. *Am J Immunol* 1:21–23
28. Carter DC, Ho JX (1994) Structure of serum albumin. *Adv Protein Chem* 45:153–203
29. Gao H, Lei L, Liu J, Kong Q, Chen X, Hu Z (2004) The study on the interaction between human serum albumin and a new reagent with antitumour activity by spectrophotometric methods. *J Photochem Photobiol A Chem* 167:213–221
30. Rub MA, Khan JM, Yaseen Z, Khan RH (2012) Conformational changes of serum albumin upon complexation with amphiphilic drug imipramine hydrochloride. *J Proteins Proteome* 3:207–215
31. Suh D, Chaires JB (1995) Criteria for the mode of binding of DNA binding agents. *Bioorg Med Chem* 3:723–728
32. Dhara K, Roy P, Ratha J, Manassero M, Banerjee P (2007) Synthesis, crystal structure, magnetic property and DNA cleavage activity of a new terephthalate-bridged tetranuclear copper (II) complex. *Polyhedron* 26:4509–4517
33. Boger DL, Fink BE, Brunette SR, Tse WC, Hedrick MP (2001) A simple, high-resolution method for establishing DNA binding affinity and sequence selectivity. *J Am Chem Soc* 123:5878–5891